Catalytic Hydrolysis of Adenosine 2′,3′-Cyclic Monophosphate by Cu^{II} Terpyridine

Lisa A. Jenkins,† James K. Bashkin,*,† Jennifer D. Pennock,† Jan Florián,‡ and Arieh Warshel‡

Department of Chemistry, Washington University, Box 1134, 1 Brookings Drive, St. Louis, Missouri 63130-4899, and Department Chemistry, University of Southern California, Los Angeles, California 90089-1062

Received February 24, 1999

The hydrolysis and transesterification of RNA are catalyzed by a variety of metal ions, metal complexes, metalloenzymes, and ribozymes. These reactions are of fundamental biochemical importance. However, the role that metal ions play in RNA hydrolysis is not completely understood. We previously showed that aqueous Cu(II) terpyridine (Cutrpy) is effective for both transesterification and hydrolysis of RNA, and we harnessed this reactivity by constructing ribozyme mimics that employ terpyridyl Cu(II) in their active sites. Here we report a detailed kinetic study of the hydrolysis of adenosine-2′,3′-cyclic monophosphate (cAMP) by Cutrpy. The reaction is established to be first-order in Cutrpy and first-order in substrate. Catalytic turnover is observed, although product inhibition occurs. Chloride ion also inhibits the reaction, which indicates the disadvantage of using NaCl as an ionic strength buffer in related studies. The pH−rate profile is sigmoidal and implicates the hydroxide form of the catalyst, $CutrpyOH^+$, as the active species. Isotope effects were used to determine whether the metal hydroxide acts as a nucleophile or a base. The solvent deuterium kinetic isotope effect, k_H/k_D, was measured to be 1.0 ± 0.1 after considering equilibrium isotope effects. To assist the mechanistic interpretation of the measured isotope effects, the fractionation factors for a dianionic phosphorane transition state (methyl phosphate dianion) and hydroxide were evaluated by ab initio quantum chemical calculations. Considering the calculated results along with the relevant experimental fractionation factors, isotope effects were predicted for three overall mechanisms: nucleophilic catalysis, general base catalysis, and specific base/general acid catalysis. We conclude that $CutrpyOH^+$ acts as a nucleophilic catalyst in the hydrolysis of cAMP. This contrasts with the behavior of $CutrpyOH^+$ as a base catalyst in the transesterification of RNA.

Introduction

Dialkyl phosphate esters form the anionic backbone of the nucleic acids DNA and RNA, and the hydrolytic breakdown of these esters is of fundamental chemical and biochemical importance. Both transesterification and hydrolysis are important routes for the scission of nucleic acids. Under mild conditions, DNA is generally inert to hydrolysis in the absence of nuclease enzymes.[1−3] However, some examples of metal-mediated DNA hydrolysis have been reported.[4−13] Hydrolytic RNA cleavage often occurs by initial transesterification, giving a 5′-OH and a strained five-membered ring, 2′,3′-cyclic phosphate, which hydrolyzes in a subsequent step (Figure 1).[14] Metal ions play important roles in many enzyme- and all ribozyme-mediated examples of these scission reactions.[15−19] Both "free metal ions" and well-defined complexes [15,20−26] have been reported to cleave RNA by this transesterification−hydrolysis route.

Most studies on hydrolytic RNA cleavage have concentrated on the transesterification reaction, although Kuusela and Lönnberg have elegantly described the metal-ion catalyzed hydrolysis of RNA and 2′,3′-cyclic phosphates.[27,28] The Hamilton group has also recently described the hydrolysis of cAMP by Cutrpy

* Corresponding authors. Tel.: (314) 935-4801. Fax: (314) 935-4481. E-mail: bashkin@wuchem.wustl.edu.
† Washington University.
‡ University of Southern California.

(1) Westheimer, F. H. *Science* **1987**, *235*, 1173−1178.
(2) Trawick, B. N.; Daniher, A. T.; Bashkin, J. K. *Chem. Rev.* **1998**, *98*, 939−960.
(3) Bashkin, J. K. *Chem. Rev.* **1998**, *98*(3), 937.
(4) Basile, L. A.; Raphael, A. L.; Barton, J. K. *J. Am. Chem. Soc.* **1987**, *109*, 7550.
(5) Hegg, E. L.; Burstyn, J. N. *Inorg. Chem.* **1996**, *35*, 7474−7481.
(6) Takasaki, B. K.; Chin, J. *J. Am. Chem. Soc.* **1993**, *115*, 9337−9338.
(7) Takasaki, B. K.; Chin, J. *J. Am. Chem. Soc.* **1994**, *116*, 1121−1122.
(8) Takasaki, B. K.; Chin, J. *J. Am. Chem. Soc.* **1995**, *117*, 8582−8585.
(9) Chin, J. *Curr. Opin. Chem. Biol.* **1997**, *1*, 514−521.
(10) Komiyama, M.; Kodama, T.; Takeda, N.; Sumaoka, J.; Shiiba, T.; Matsumoto, Y.; Yashiro, M. *J. Biochem.* **1994**, *115*, 809−810.
(11) Komiyama, M.; Takeda, N.; Takahashi, Y.; Uchida, H.; Shiiba, T.; Kodama, T.; Yasiro, M. *J. Chem. Soc., Perkin Trans. 2* **1995**, 269−274.
(12) Schnaith, L. M. T.; Hanson, R. S.; Que, L. J. *Proc. Natl. Acad. Sci. U.S.A.* **1994**, *91*, 569−573.
(13) Kimball, A. S.; Lee, J.; Jayaram, M.; Tullius, T. D. *Biochemistry* **1993**, *32*, 4698−4701.
(14) Perreault, D. M.; Anslyn, E. V. *Angew. Chem., Int. Ed. Engl.* **1997**, *36*, 433−450.
(15) Bashkin, J. K.; Jenkins, L. A. *Comments Inorg. Chem.* **1994**, *16*, 77−93.
(16) Zhou, D.-M.; Taira, K. *Chem. Rev.* **1998**, *98*(3), 991−1026.
(17) Cowan, J. A. *Chem. Rev.* **1998**, *98*(3), 1067−1087.
(18) Kuimelis, R. G.; McLaughlin, L. W. *Chem. Rev.* **1998**, *98*(3), 1027−1044.
(19) Wilcox, D. E. *Chem. Rev.* **1996**, *96*, 2435−2458.
(20) Dimroth, K.; Witzel, H.; Huelsen, W.; Mirbach, W. *Annalen.* **1959**, *620*, 94−108.
(21) Butzow, J. J.; Eichhorn, G. L. *Nature* **1975**, *254*, 358.
(22) Stern, M. K.; Bashkin, J. K.; Sall, E. D. *J. Am. Chem. Soc.* **1990**, *112*, 5357.
(23) Breslow, R.; Huang, D.-L. *Proc. Natl. Acad. Sci. U.S.A.* **1991**, *88*, 4080−4083.
(24) Shelton, V. M.; Morrow, J. R. *Inorg. Chem.* **1991**, *30*, 4295−4299.
(25) Morrow, J. R.; Shelton, V. M. *New J. Chem.* **1994**, *18*, 371−375.
(26) Kuusela, S.; Lönnberg, H. *Curr. Top. Solution Chem.* **1997**, *2*, 29−47.
(27) Kuusela, S.; Lönnberg, H. *J. Phys. Org. Chem.* **1993**, *5*, 347−356.
(28) Kuusela, S.; Lönnberg, H. *Nucleosides Nucleotides* **1996**, *15*, 1669−1678.

10.1021/ic990228r CCC: $18.00
Published on Web 06/11/1999

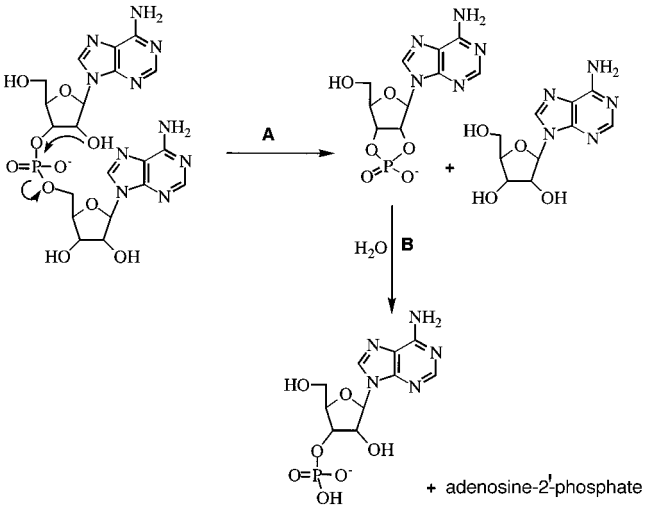

Figure 1. Transesterification (A) of the RNA dimer ApA and hydrolysis (B) of adenosine-2′,3′-cyclic phosphate.

analogues.[29] However, as Bruice and Dempcy have noted, the hydrolysis of dialkyl phosphate esters by metal catalysts has received much less attention than the hydrolysis of mono- and triesters.[30] Furthermore, model aryl phosphate esters such as bis(*p*-nitrophenyl)phosphate have received far more attention than their alkyl counterparts.[31−36] The focus on aryl substrates derives from an interest in detoxifying herbicides [37] and chemical warfare agents,[38] but is also driven by the relative ease of analysis: aryl phosphates tend to cleave much faster than alkyl phosphates, and the release of aryloxide leaving groups is amenable to study by UV/vis spectroscopy. However, there are substantial differences in the hydrolyses of aryl and alkyl phosphate esters, e.g. the K_a values of the leaving groups vary by as much as 8 units. Activated esters may be poor models for nucleic acids.[39,40] Recently, Kirby and Marriott have combined the desirable features of alkyl and aryl phosphates by using an acetal ester of uridine 3′-phosphate.[41] This compound has a specially designed leaving group (with a pK_a near 11) which rapidly decomposes to *p*-nitrophenolate.

Despite the importance of metal-catalyzed hydrolysis of true DNA and RNA substrates,[26] many mechanistic aspects of these reactions are unresolved. As part of our investigation of hydrolytic RNA cleavage and the design of functional mimics of ribozymes,[2,15,22,40,42−54] we report here a detailed kinetic study of the catalytic hydrolysis of adenosine 2′,3′-cyclic-monophosphate (cAMP) by Cu(II) terpyridine (Cutrpy). A number of other groups have also reported functional mimics of ribozymes.[2,55−63] Here we provide evidence that a single Cutrpy interacts with one cAMP substrate in the rate-determining step of hydrolysis, and that a Cutrpy-bound hydroxide is the reactive catalyst. We use solvent isotope effects to conclude that the Cutrpy-bound hydroxide acts as a nucleophile and not as a general base. A preliminary report of this work has been published.[40]

Experimental and Computational Procedures

Materials. Adenosine 2′,3′-cyclic monophosphate, 2′- and 3′-monophosphates, adenosine, adenine, *p*-toluenesulfonic acid, and KH_2PO_4 were purchased from Sigma and used as received. Copper terpyridine was prepared by heating a 1:1 mixture of $CuCl_2$ and 2,2′:6′, 6″-terpyridine to boiling in water. Slow cooling yielded dark green-blue crystals whose identity was confirmed by comparison of its solution UV/vis spectrum to that in the literature,[64] as well as by mass spectrometry. HEPES, EPPS, and CHES buffers were purchased from Sigma. Fisher HPLC grade water was used for all solutions. Diethylpyrocarbonate (DEPC) was purchased from Sigma.

HPLC Assay. An analytical method was adapted from that of Morrow.[24] Separation of reactants and products was achieved on either a Supelcosil LC-18 or Whatman Equivalent C-18 reversed phase analytical column (4.6 mm × 25 cm) using a solvent delivery system coupled to a UV/vis detector and an autoinjector. Waters Maxima software was used to run the instrument and integrate chromatograms. Mobile phase solvent A (10 mM KH_2PO_4, pH unadjusted) was mixed isocratically with solvent B (60% MeOH in H_2O) in a ratio of 80/20, and a flow rate of 1 mL/min was used. *p*-Toluenesulfonic acid (pTSA) was used as an internal standard.

(29) Liu, S.; Luo, Z.; Hamilton, A. D. *Angew. Chem., Int. Ed. Engl.* **1997**, *36*, 2678−2680.
(30) Dempcy, R. O.; Bruice, T. C. *J. Am. Chem. Soc.* **1994**, *116*, 4511−4512.
(31) Burstyn, J. N.; Deal, K. A. *Inorg. Chem.* **1993**, *32*, 3585−3586.
(32) Morrow, J. R.; Buttrey, L. A.; Berback, K. A. *Inorg. Chem.* **1992**, *31*, 1, 16−20.
(33) Morrow, J. R.; Trogler, W. C. *Inorg. Chem.* **1988**, *27*, 3387−94.
(34) Deal, K. A.; Hengge, A. C.; Burstyn, J. N. *J. Am. Chem. Soc.* **1996**, *118*, 1713−18.
(35) Hengge, A. C.; Tobin, A. E.; Cleland, W. W. *J. Am. Chem. Soc.* **1995**, *117*, 5919−26.
(36) Roigk, A.; Hettich, R.; Schneider, H.-J. *Inorg. Chem.* **1998**, *37*, 751−756.
(37) Breslow, R.; Singh, S. *Bioorg. Chem.* **1988**, *16*, 408−417.
(38) Yang, Y.-C.; Baker, J. A.; Ward, J. R. *Chem. Rev.* **1992**, *92*, 1729−1743.
(39) Menger, F. M.; Ladika, M. *J. Am. Chem. Soc.* **1987**, *109*, 3145−3146.
(40) Bashkin, J. K.; Jenkins, L. A. *J. Chem. Soc., Dalton Trans.* **1993**, 3631−2.
(41) Kirby, A. J.; Marriott, R. E. *J. Am. Chem. Soc.* **1995**, *117*, 833−834.
(42) Bashkin, J. K.; Gard, J. K.; Modak, A. S. *J. Org. Chem.* **1990**, *55*, 5125.
(43) Modak, A. S.; Gard, J. K.; Merriman, M. C.; Winkeler, K. A.; Bashkin, J. K.; Stern, M. K. *J. Am. Chem. Soc.* **1991**, *113*, 283.
(44) Bashkin, J. K.; McBeath, R. J.; Modak, A. S.; Sample, K. R.; Wise, W. B. *J. Org. Chem.* **1991**, *56*, 3168.
(45) Bashkin, J. K. In *Bioinorganic Chemistry of Copper*; Karlin, K. D., Tyeklar, Z., Eds.; Chapman and Hall: New York, 1993; pp 132−139.
(46) Bashkin, J. K.; Sondhi, S. M.; Sampath, U.; d'Avignon, D. A.; Modak, A. S. *New J. Chem.* **1994**, *18*, 305−316.
(47) Bashkin, J. K.; Frolova, E. I.; Sampath, U. *J. Am. Chem. Soc.* **1994**, *116*, 5981−5982.
(48) Bashkin, J. K.; Sampath, U. S.; Frolova, E. I. *Appl. Biochem. Biotechnol.* **1995**, *54*, 43−56.
(49) Bashkin, J. K.; Xie, J.; Daniher, A. T.; Sampath, U.; Kao, J. L.-F. *J. Org. Chem.* **1996**, *61*, 2314−2321.
(50) Bashkin, J. K.; Xie, J.; Daniher, A. T.; Jenkins, L. A.; Yeh, G. C. In *DNA and RNA Cleavers and Chemotherapy of Cancer and Viral Diseases*; Meunier, B., Ed.; Kluwer: The Netherlands, 1996; pp 355−366.
(51) Jenkins, L. A.; Bashkin, J. K.; Autry, M. E. *J. Am. Chem. Soc.* **1996**, *118*, 6822−6825.
(52) Jenkins, L. A.; Bashkin, J. K. *Inorg. Chim. Acta* **1997**, *263*, 49−52.
(53) Daniher, A. T.; Xie, J.; Mathur, S.; Bashkin, J. K. *Bioorg. Med. Chem.* **1997**, *5*, 1037−1042.
(54) Daniher, A. T.; Bashkin, J. K. *J. Chem. Soc., Chem. Commun.* **1998**, 1077−1078.
(55) Reynolds, M. A.; Beck, T. A.; Say, P. B.; Schwartz, D. A.; Dwyer, B. P.; Daily, W. J.; Vaghefi, M. M.; Metzler, M. D.; Klem, R. E.; Arnold, L. J., Jr. *Nucleic Acids Res.* **1996**, *24*, 760−765.
(56) Huesken, D.; Goodall, G.; Blommers, M. J. J.; Jahnke, W.; Hall, J.; Haener, R.; Moser, H. E. *Biochemistry* **1996**, *35*, 16591−16600.
(57) Hall, J.; Huesken, D.; Haener, R. *Nucleic Acids Res.* **1996**, *24*, 3522−3526.
(58) Hall, J.; Huesken, D.; Pieles, U.; Moser, H. E.; Haener, R. *Chem. Biol.* **1994**, 185−190.
(59) Hovinen, J.; Guzaev, A.; Azhayeva, E.; Azhayev, A.; Lönnberg, H. *J. Org. Chem.* **1995**, *60*, 2205−2209.
(60) Komiyama, M.; Inokawa, T.; Yoshinari, K. *J. Chem. Soc., Chem. Commun.* **1995**, 77−78.
(61) Matsumura, K.; Endo, M.; Komiyama, M. *J. Chem. Soc., Chem. Commun.* **1994**, 2019−2020.
(62) Magda, D.; Miller, R. A.; Sessler, J. L.; Iverson, B. L. *J. Am. Chem. Soc.* **1994**, *116*, 7439−7440.
(63) Magda, D.; Crofts, S.; Lin, A.; Miles, D.; Wright, M.; Sessler, J. L. *J. Am. Chem. Soc.* **1997**, *119*, 2293−2294.
(64) Harris, C. M.; Lockyer, T. N. *Aust. J. Chem.* **1970**, *23*, 673−682.

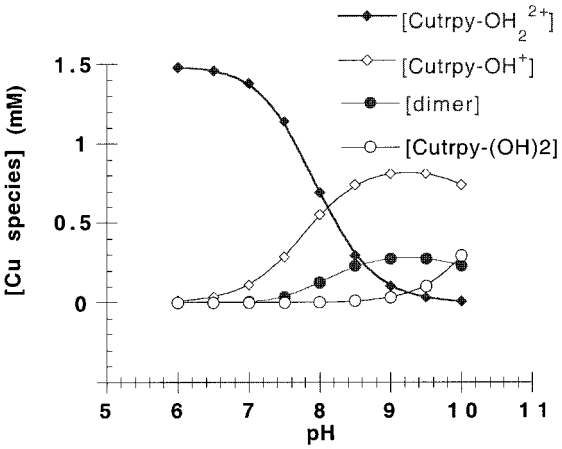

Figure 2. Speciation diagram of Cu(II) terpyridine species in aqueous solution as a function of pH at ionic strength 0.1 M and $[Cutrpy]_{total}$ = 1.5 mM (calculated from published equilibrium constants).

All reactions were run in autoclaved 1.5-mL microcentrifuge tubes at a total volume of 0.5, 1.0, or 1.5 mL. All water was treated with 0.1% DEPC and autoclaved at 121 °C for 40 min, and gloves were worn in all stages of preparation. Stock solutions of all reactants were prepared in water and stored at ~5 °C. The pH values of the pTSA, $NaClO_4$, and Cutrpy solutions were adjusted to 7 before use. Reaction mixtures were prepared from the stock solutions using micro-pipets. Upon addition of cAMP to the mixtures, the tubes were closed and shaken, and aliquots taken as time zero points. The tubes were then incubated at 37 °C in a circulating water bath. Aliquots were removed, quenched with EDTA, and injected into the HPLC. The pH measurements were done at 37 °C with a Corning PS30 Check-mite pH sensor which was calibrated at 37 °C. Measurements were made at least twice during the reactions, and reported pH's are arithmetic averages of those measurements. The products of the reaction, 2′-AMP and 3′-AMP, were verified by comparison of HPLC retention times with authentic standards. At longer times (>10% reaction) adenosine also appeared as a product.

Kinetics. Dependence of Rate Constants on [Cutrpy]. Because of product inhibition, analyses were done using initial rates. Reaction mixtures contained 0.1 mM cAMP, 4 mM pTSA, 50 mM $NaClO_4$ (total ionic strength: 0.056 M), 5 mM HEPES buffer (pH = 7.4 and 8.2; the pK_a of HEPES is 7.5 at 25 °C), and 0.25−2.5 mM Cutrpy. At least five aliquots of the reaction were quenched with EDTA and analyzed by HPLC over approximately 30−60% of the reaction to yield a concentration vs time dependence. The data were fit to exponential decays ($r > 0.99$); all reactions were done at least in triplicate and k_{obs} values are reported as means ± 1 sample standard deviation. The error bars on linear plots of k_{obs} (Figures 3B, 4, and 6) and initial rate (Figure 5) indicate ± 1 sample standard deviation. The first derivatives of the exponential decays at $t = 0$ were used to obtain initial rates. Conversions from HPLC area ratio units to concentration units were accomplished by using time-zero ratios of cAMP HPLC peak area-to-pTSA HPLC peak area as calibrations.

Dependence of Rate Constants on pH. Reaction mixtures were the same as above except that EPPS (pK_a = 8.0 at 25 °C) or CHES (pK_a = 9.3 at 25 °C) buffers were also used, the concentration of $NaClO_4$ was adjusted with changing buffer ratio so as to maintain constant ionic strength, and the concentration of Cutrpy was fixed at either 1.0 or 1.5 mM.

Dependence of Initial Rate on [cAMP]. Reaction mixtures were similar to those described above. The concentration of Cutrpy was fixed at 1.0 mM. The concentration of cAMP was varied from 0.030 to 5.0 mM. The studies were done at pH 7.4 and ionic strength 0.056 M (data not shown), and pH 8.2 at two ionic strengths: 0.056 and 0.50 M (Figure 5). The initial rates were corrected for background (buffer) hydrolysis at higher $[cAMP]_o$ using the average observed background initial rate constant. At very high concentrations of cAMP (>20 mM), it became difficult to resolve substrate, product and internal standard HPLC peaks from small impurities in the cAMP.

Isotope Effect. Standard solutions of all reactants and buffers were prepared in 99.9% D_2O, and pH adjusted with NaOH dissolved in D_2O or acetic acid diluted in D_2O. These solutions were used to prepare reaction mixtures which were diluted with D_2O under conditions similar to the [cAMP] dependence studies. The pH of the reaction mixtures was measured directly, and converted to pD by adding 0.4.[65]

Curve Fitting. Linear least-squares analysis was performed using the program EZFIT,[66] and speciation distributions using the program SPE.[67] Errors in fits are reported as standard deviations.

Ab Initio Methods. Fractionation factors (Φ)[68] for model compounds were calculated from the gas-phase thermal free energies (G) using the formula

$$\Phi(\mathrm{AH}) = \exp\left\{-\frac{G(\mathrm{H_2O}) + G(\mathrm{AD}) - G(\mathrm{DHO}) - G(\mathrm{AH})}{RT}\right\} \quad (1)$$

where R is the universal gas constant and $T = 298$ K. The thermal free energies were evaluated as a sum of the vibrational, rotational, and translational contributions to the standard free energy using the ideal gas, rigid-rotor, and harmonic approximations.[69] Harmonic vibrational frequencies were determined by the HF/6-31G* method at the geometries that were fully optimized at the same computational level. Ab initio calculations were carried out using the Gaussian94 program.[70]

Results/Discussion

The hydrolysis of cAMP is promoted by Cutrpy at biological pH although Cutrpy does not promote the hydrolysis of bis(*p*-nitrophenyl) phosphate, a compound sometimes used as a model of RNA. The failure to hydrolyze bis(*p*-nitrophenyl) phosphate was originally reported by Morrow and Trogler[33] and discussed by Shelton and Morrow.[24] We confirmed this result in our own laboratory by the direct comparison of the rates of bis(*p*-nitrophenyl)phosphate hydrolysis in the presence and absence of Cutrpy.[40] In fact, under our conditions, Cutrpy *inhibited* the buffer-catalyzed cleavage of bis(*p*-nitrophenyl)phosphate (the reaction was reproducibly slower in the presence of Cutrpy than in its absence).

The dependence of cAMP hydrolysis on both pH and [Cutrpy] was consistent with the hydroxide form of the Cutrpy, Cutrpy-OH^+, being the active catalyst. The reaction is first-order in both Cutrpy and cAMP and is second-order overall. The solvent isotope effect is consistent with the hydroxide bound to Cutrpy acting as a nucleophile (vide infra).

The hydrolysis of cAMP by Cutrpy yields 2′-AMP and 3′-AMP as products, and ultimately adenosine (and therefore inorganic phosphate). Because the cAMP stock solutions are stable (no detectable decomposition over several months) and the 2′- and 3′-AMP stock solutions rapidly decompose to adenosine, the adenosine reaction product is likely derived from the initial 2′- and 3′-AMP products via a dephosphorylation

(65) Schowen, K. B.; Schowen, R. L. *Methods Enzymol.* **1982**, *87*, 551−607.
(66) Noggle, J. H. *Practical Curve Fitting and Data Analysis*; PTR Prentice-Hall: Englewood Cliffs, NJ, 1993.
(67) Martell, A. E.; Motekaitis, R. J. *Determination and Use of Stability Constants*, 2nd ed.; VCH Publishers: New York, 1992.
(68) Lowry, T. H.; Richardson, K. S. *Mechanism and Theory in Organic Chemistry*, 3rd ed.; Harper and Row: New York, 1987.
(69) McQuarrie, D. A. *Statistical Mechanics*; Harper and Row: New York, 1976.
(70) Frisch, M. J.; Trucks, G. W.; Schlegel, H. B.; Gill, P. M. W.; Johnson, B. G.; Robb, M. A.; Cheeseman, J. R.; Keith, T.; Petersson, G. A.; Montgomery, J. A.; Raghavachari, K.; Al-Laham, M. A.; Zakrzewski, V. G.; Ortiz, J. V.; Foresman, J. B.; Cioslowski, J.; Stefanov, B. B.; Nanayakkara, A.; Challacombe, M.; Peng, C. Y.; Ayala, P. Y.; Chen, W.; Wong, M. W.; Andres, J. L.; Replogle, E. S.; Gomperts, R.; Martin, R. L.; Fox, D. J.; Binkley, J. S.; Defrees, D. J.; Baker, J.; Stewart, J. P.; Head-Gordon, M.; Gonzalez, C.; Pople, J. A. *Gaussian 94*, Revision D.2; Gaussian, Inc.: Pittsburgh, PA, 1995.

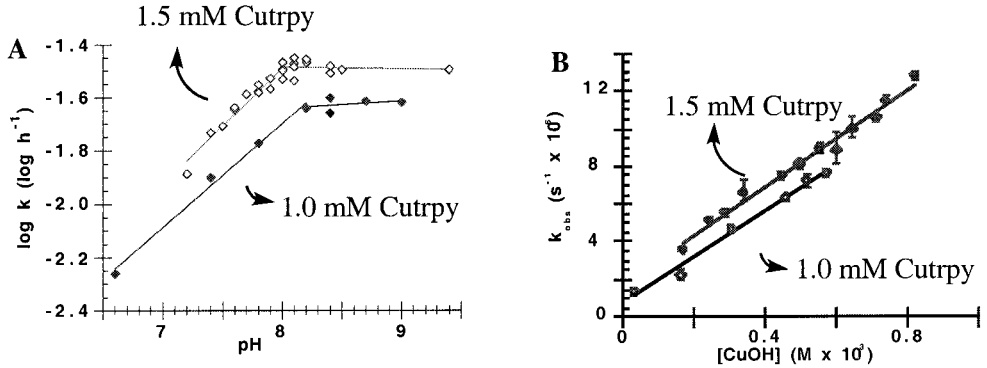

Figure 3. Dependence of k_{obs} for the hydrolysis of cAMP by Cutrpy on pH. The experiments at 1.0 mM Cutrpy utilized a combination of HEPES and CHES buffers, while those at 1.5 mM Cutrpy used only EPPS buffer. (A) $[Cutrpy]_{total} = 1.0$ mM and 1.5 mM. Rate constants were corrected for background hydrolysis at pH > 8.2 by subtracting control rate constants from Cutrpy rate constants. Each pH profile contains two distinct linear regions. These separate regions were fit by linear least squares using the program EZFIT, and the intersections of the lines were determined mathematically. The intersections, corresponding to the points of kinetic saturation, are at pH 8.2 and 8.3 for data collected at 1.5 and 1.0 mM Cutrpy, respectively. (B) k_{obs} vs [Cutrpy-OH$^+$] as derived from the (uncorrected) pH profile. [Cutrpy-OH] was calculated as described in the text. The intercepts of the plots, determined from linear least squares, are $(1.9 \pm 0.3) \times 10^{-6}$ s^{-1} at $[Cutrpy]_{total} = 1.5$ mM, and $(1.4 \pm 0.2) \times 10^{-6}$ s^{-1} at $[Cutrpy]_{total} = 1.0$ mM. This is consistent with a small amount of background (buffer) hydrolysis.

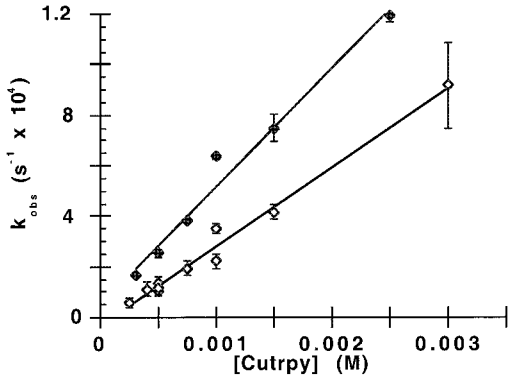

Figure 4. Dependence of k_{obs} for the hydrolysis of cAMP on [Cutrpy] at pH 7.4 (filled diamonds) and 8.2 (open diamonds).

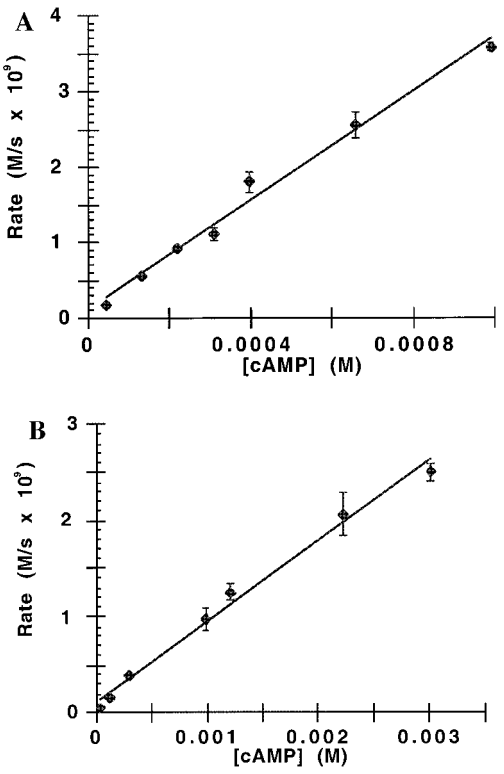

Figure 5. Dependence of the initial rate (IR) of cAMP hydrolysis on [cAMP] in 99.9% D_2O. (A) Kinetics at pD = 8.2. (B) Kinetics at pD = 7.4. The slopes of the lines, which are equivalent to k_{obs} according to eq 1, are $(3.6 \pm 0.2) \times 10^{-6}$ s^{-1} at pD 8.2, and $(8.3 \pm 0.3) \times 10^{-7}$ s^{-1} at pD 7.4. The *y* intercepts are negligible: $(1.1 \pm 0.8) \times 10^{-10}$ M s^{-1} at pD 8.2 and $(1.1 \pm 0.5) \times 10^{-10}$ M s^{-1} at pD 7.4.

reaction. Lönnberg and co-workers have reported a similar process in the hydrolysis of 2′,3′-cUMP by metal ions.[27]

The hydrolysis of cAMP by Cutrpy was studied in HEPES and EPPS buffers, but there were two disadvantages to using HEPES. Slight inhibition of the Cutrpy-catalyzed reaction was observed with increasing [HEPES] from 5 to 20 mM, while no such inhibition was observed in EPPS over the same concentration range. In addition, background (buffer) hydrolysis rates were higher in HEPES than in EPPS.

The reaction was completely inhibited in 50 mM NaCl. A similar inhibition was seen in phosphate buffers. We believe that chloride and phosphate bind to the copper and prevent substrate binding. This has important implications for the choice of experimental conditions, and may preclude the use of copper reagents in vivo. It certainly has important implications for the choice of pH and ionic strength buffers used in kinetic studies. No inhibition was observed with $NaClO_4$, so sodium ion was an innocent spectator, and we used $NaClO_4$ as an ionic strength buffer. At concentrations of Cutrpy above 2.5 mM, precipitates formed. At pH 7.4, $[cAMP]_o = 0.1$ mM, there was no significant difference in rate between 0.25 mM Cutrpy and 0.25 mM $CuCl_2$ (initial rates were $(5.8 \pm 0.2) \times 10^{-11}$ and $(5.56 \pm 0.08) \times 10^{-11}$ M/s, respectively). However, it is likely that at this pH, a large fraction of the "free" Cu^{2+} was precipitated. Attempts to study the hydrolysis of cAMP by "free" Cu^{2+} at concentrations above 0.25 mM and at pH above 7.4 resulted in the formation of visible copper precipitates. The trpy ligand clearly allows the inherent hydrolytic activity of Cu(II) to be accessed over a wide pH range not available to the free metal ion.

Catalytic turnover was demonstrated by the hydrolysis of 2.5 mM cAMP with 1.0 mM Cutrpy. At least 2 turnovers were observed over 10 days. However, the observed rate decreased as a function of time, and we investigated the possibility of inhibition by the reaction products. Inhibition by 0.5 mM inorganic phosphate was observed, as discussed above. The 3′-phosphate and 2′-phosphate monoester products did not inhibit the reaction at or below concentrations of 0.25 mM.

Cu(II) terpyridine consists of four major species in aqueous solution. These are the aquo-Cutrpy (Cutrpy-OH_2^{2+}), the hydroxo species (Cutrpy-OH^+), the bis-hydroxo species (Cutrpy-$(OH)_2$), and the hydroxy-bridged dimer ((Cutrpy-$OH)_2^{2+}$). These equilibria have been described by Cali et al.,[71] and the speciation as a function of pH is depicted in Figure 2. Similar speciation was reported by Morrow and Trogler[33] for the related complex, copper(II) bipyridine.

Rate of Hydrolysis of cAMP by Cutrpy is pH-Dependent. We used this dependence to help determine the reactive Cutrpy species. As shown in Figure 3, the initial rate constant increased as a function of pH, reaching a maximum near pH 8.2. The data are consistent with the existence of a titratable proton on the Cutrpy, the curve reaching a maximum at the pH where the [Cutrpy-OH^+] is maximal. Similar profiles were obtained in two buffer systems and at different total concentrations of Cutrpy. Our data are also consistent with the reported pK_a for Cutrpy-OH_2^{2+} of 8.08.[71]

Examination of Figure 2, however, reveals that the formation of the dimer also parallels the increase in k_{obs} as a function of pH. The dependence of k_{obs} on [Cutrpy] was used to rule out the dimer, and to confirm Cutrpy-OH^+, as the reactive species. This is described in the following section.

Reaction is First-Order in Cutrpy. The dependence of k_{obs} on [Cutrpy] is shown in Figure 4. Plots of k_{obs} vs [Cutrpy] are linear at pH 7.4 and 8.2 and are consistent with a first-order dependence on one of the Cutrpy species in solution. There is no difference in the apparent order of the reaction with respect to Cutrpy at these two pH values, and the *y* intercepts are zero, indicating that hydrolysis due to buffer is negligible. Further confirmation of this first-order dependence is seen in the plots of log k_{obs} vs log [Cutrpy], which are linear with slopes of 1.

Interestingly, plots of (log k_{obs}) vs the log[concentration] for any of the major Cutrpy species give reaction orders (slopes) which parallel the stoichiometry of the species in equilibrium. Thus, the log−log plot of k_{obs} vs [Cutrpy-OH_2^{2+}] has a slope of 1, as do similar plots for k_{obs} vs [Cutrpy-$(OH)_2$] and [Cutrpy-OH^+]. The corresponding log−log plot of k_{obs} vs hydroxide-bridged dimer concentration shows a half-order dependence. This was expected, since equilibration between Cu(II) species is likely to occur faster than the hydrolysis reaction,[34] and it is consistent with the Curtin−Hammett principle.[72] Since the reaction is first-order in [Cutrpy-OH^+] and half-order with respect to the dimer, the Cutrpy-OH^+ must be the important reactive species. We would expect a first-order dependence on the [dimer] and second-order dependencies on the monomeric complexes if the dimer were the reactive species. Plotting k_{obs} vs [Cutrpy-OH^+] gives a line with a slope equal to the second-order rate constant, k_2, according to eqs 2 and 3. The k_2 values at $[Cutrpy]_{total} = 1.0$ mM and pH 7.4 and 8.2 are $(9.4 \pm 0.6) \times 10^{-3}$ and $(1.4 \pm 0.1) \times 10^{-2}$ M^{-1} s^{-1}, respectively.

$$\text{rate} = \frac{-d[\text{cAMP}]}{dt} = k_{obs}\,[\text{cAMP}] \qquad (2)$$

$$k_{obs} = k_2\,[\text{Cutrpy-OH}^+] \qquad (3)$$

Dependence of the Rate on [cAMP]. These studies were carried out with total [Cutrpy] = 1.0 mM and ionic strength 0.056 M. The results were linear and consistent with first-order dependence in [cAMP] (data not shown, but analogous plots from experiments run in D_2O are shown in Figure 5). However, the corresponding log−log plot (not shown) for initial rate vs [cAMP] gave lines with slopes of 0.96 ± 0.03 and 0.85 ± 0.03 at pH 8.2 and 7.4, respectively. Reaction orders of slightly less than 1 with respect to substrate have been observed previously in RNA transesterification chemistry; this may be consistent with binding of the Cutrpy to nonproductive sites on the cAMP (the adenosine moiety, for instance).[24,52] An additional study of initial rate vs [cAMP] was done at a much higher ionic strength (0.5 M). This too showed linear behavior, but a decreased slope vs the 0.056 M ionic strength data which is consistent with two oppositely charged species interacting in the activated complex. The slopes of the least-squares lines for initial rate vs [cAMP] are equivalent to k_{obs} according to eq 1. At pH 8.2, the slope is $(2.9 \pm 0.1) \times 10^{-6}$ s^{-1} at an ionic strength of 0.056 and $(2.1 \pm 0.1) \times 10^{-6}$ s^{-1} at an ionic strength of 0.5. Thus, we conclude that one cAMP moiety reacts with one Cutrpy moiety to form the activated complex for this reaction.

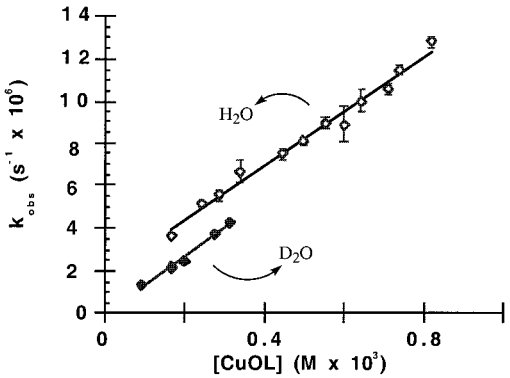

Figure 6. Solvent isotope effect for the hydrolysis of cAMP by Cutrpy. The slopes of the lines, equivalent to k_2, are $(1.28 \pm 0.05) \times 10^{-2}$ and $(1.33 \pm 0.08) \times 10^{-2}$ M^{-1} s^{-1} in H_2O and D_2O respectively. The resulting isotope effect is 1.0 ± 0.1. Reaction conditions were identical (1.5 mM $[Cutrpy]_{total}$, 5 mM EPPS buffer, ionic strength = 0.056 M ($NaClO_4$)) except for the solvent being either H_2O or D_2O. Neither the H_2O nor D_2O data were corrected for background hydrolysis: the *y* intercept of $(1.9 \pm 0.3) \times 10^{-6}$ s^{-1} from the H_2O fit indicates that a negligible amount of background cleavage occurs. The *y* intercept of the line through the D_2O data is zero within experimental error.

Solvent Isotope Effect and Mechanistic Conclusions. The solvent isotope effect and subsequent mechanistic conclusions were calculated and developed in a series of steps. These steps are summarized here, and are detailed in the following sections. First, we estimated a value of the pK_a for Cutrpy-OD_2^{2+}. From this, we accounted for the equilibrium isotope effect by explicitly calculating the concentrations of Cu-aquo and hydroxo species in H_2O and D_2O, and determined the actual kinetic solvent isotope effect. Predicted isotope effects were then calculated for three possible mechanisms using fractionation factor theory. This process involved determination of fractionation factors for species in our system, and estimation of the position along the reaction coordinate at which the transition state occurs. Finally, comparison of our predicted isotope effects with the measured effect allowed mechanistic conclusions to be made.

Determination of pK_{a,D_2O} and the ratio $k_{2,H_2O}/k_{2,D_2O}$. Cutrpy-OH^+ is the reactive Cutrpy species, but it is important to determine its role as either a general base or a source of nucleophilic hydroxide. We used the solvent isotope effect to distinguish between these possibilities. The dependence of the initial rate on [cAMP] in D_2O at pD 7.4 and 8.2 is shown in Figure 5: the reaction is first order with respect to substrate as it was in H_2O. Figure 6 illustrates the dependence of k_{obs} on

(71) Cali, R.; Rizzarelli, E.; Sammartano, S.; Siracusa, G. *Transition Met. Chem.* **1979**, *4*, 328−332.
(72) Zefirov, N. S. *Tetrahedron* **1977**, *33*, 2719−2722.

[Cutrpy-OL^+] in H_2O and D_2O, as derived from the pL profiles (pL being either pH or pD). As with [cAMP], there is no change in the reaction order with respect to [Cutrpy-OL^+] upon changing to D_2O solvent. Precipitates formed at pD > 8.3 and 37 °C. After several weeks at ~5 °C, precipitates formed in the Cutrpy/D_2O stock solution. Reaction mixtures above pD 8.0 showed the formation of precipitates after several days at room temperature. The decreased solubility that we observed in D_2O hampered attempts to study the reaction over a wide catalyst concentration range.

Under conditions of equal [Cutrpy] and pL, the reaction is slowed in D_2O. The extent to which the reaction rate is affected can indicate the nature of the role of the Cutrpy-OH^+, so the ratio $k_{2,H_2O}/k_{2,D_2O}$ was needed. However, the reaction rate is pH-dependent, and rate constants must be compared either in a pL-independent region or at equivalent pL. The pK_a values of acids are usually changed in deuterium oxide solvent, so the reaction is affected in two ways: an *equilibrium* isotope effect resulting in a higher pK_a for the Cutrpy-OL_2 species in D_2O than in H_2O, and a *kinetic* solvent isotope effect. Precipitation of reactants occurred in our system at pD > 8.3, precluding comparison in a pL-independent region or a graphical determination of the pK_a of Cutrpy-OD_2^{2+}. The ΔpK_a ($pK_{a,D_2O} - pK_{a,H_2O}$) for weak acids is typically 0.5.[68] The reported value of ΔpK_a for hydrated Cu^{2+} is 0.49.[65] Since hydrated Cu^{2+} and Cutrpy have similar pK_a values (7.7 and 8.1, respectively), we used the reported ΔpK_a and estimated the pK_a for Cutrpy-OD_2^{2+} to be 8.6. A similar analysis was recently reported.[73] To determine [Cutrpy-OD^+] as a function of pH, the equilibrium constants in D_2O were estimated by adding 0.5 pK_{eq} units to the equilibrium constants reported in H_2O for any protic equilibria. The other constants were assumed to be unchanged. Thus, we were able to account for the equilibrium isotope effect by explicitly calculating [Cutrpy-OL^+] (using the program SPE[67]) and calculating k_2 from eqs 2 and 3.

Determination of the second-order rate constants from the plots in Figure 6 for $[Cutrpy]_{total} = 1.5$ mM are $(1.33 \pm 0.08) \times 10^{-2}$ M^{-1} s^{-1} in D_2O and $(1.28 \pm 0.06) \times 10^{-2}$ M^{-1} s^{-1} in H_2O. These values result in an isotope effect of 1.0 ± 0.1. We compare this with the isotope effect predicted using fractionation factor theory described below.

Fractionation Factors for Relevant Species. Fractionation factors (symbol: Φ) are equilibrium constants which measure the preference for deuterium relative to bulk water at a particular hydrogenic site.[74] Fractionation factor theory allows the prediction of secondary (equilibrium) solvent isotope effects by using eq 4, which results from explicitly expressing the ratio of the equilibrium constants in H_2O and D_2O. The equilibrium may

$$\frac{K_a^{H_2O}}{K_a^{D_2O}} = \frac{\Pi\Phi_{reactants}}{\Pi\Phi_{products}} \qquad (4)$$

be between reactants and products to calculate a equilibrium isotope effect, or between reactants and transition state to calculate a kinetic isotope effect. For a mechanism involving a proton in flight during the transition state, a large primary kinetic isotope effect will further increase the solvent isotope effect.

Values of Φ for several hydrated metal ions have been published. For instance, Φ is nearly unity for aquo Fe(III), Cr(III), and Mn(II),[74] and varies from 0.73 to 0.90 for Co(II).[75] To predict the solvent isotope effect in our system using fractionation factors, we needed to know Φ for Cutrpy-OL^+, the metal-bound hydroxide. This value will depend on whether the proton is in an environment more similar to solvent, L-O-L (Φ = 1), or more similar to lyonium, L_3O^+ (Φ = 0.69). Consistent with the reported values of Φ for Co(II) hydroxides, which range from 0.72 to 0.77,[75] we conclude that Φ for Cutrpy-OL^+ (Φ_{Cu-OL}) is somewhere in the range from 0.69 to 1, probably near 0.8.

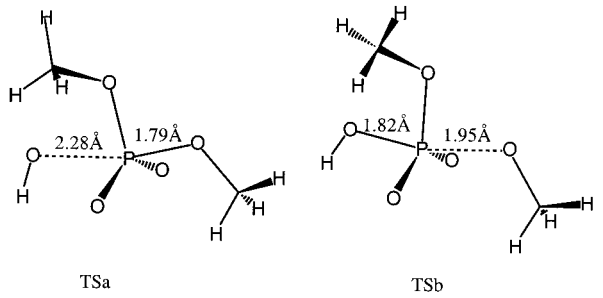

Figure 7. Structures of the dimethylphosphorane dianion that were used in the theoretical evaluation of the fractionation factor of the phosphorane−Cutrpy transition state.

Table 1. Comparison of the Calculated and Experimental Fractionation Factors

			Φ	
molecule	E_{MP2}[a]	ΔG_{solv}[b]	calcd[c]	exp
TSa[d]	−796.165653	−239.0	0.85	
TSb[d]	−796.167729	−237.3	1.04	
HPO_4^{2-}	−641.641641	−246.7	1.03	0.91[e]
OH^-	−75.602058	−110.8	0.55	0.41[f]

[a] MP2/6-31+G**/HF/6-31G* energy (au). [b] Solvation free energy (kcal/mol) calculated using the Langevin dipoles solvation model[81] implemented in the program ChemSol 1.0.[82] [c] Equation 1. [d] Figure 7. [e] Reference 74. [f] Reference 68.

Another important fractionation factor for our system is that of a phosphorane transition state (Φ_{P-OL}). To estimate the magnitude of Φ_{P-OL} we carried out ab initio calculations for the dimethylphosphorane dianion presented in Figure 7. Here, the left-hand (TSa) and right-hand (TSb) structures represent, respectively, a transition state and minimum on the gas-phase HF/6-31G* potential energy surface. However, as can be seen from the energies presented in Table 1, the TSb structure approximates more properly the transition state geometry in aqueous solution. In fact, the (P-$O_{nucleophile}$, P-$O_{leaving-group}$) section of the potential energy surface of the phosphorane dianion in aqueous solution is extremely flat.[76,77] Thus, structures presented in Figure 7 were used by us to estimate the uncertainty of the calculated fractionation factor due to the uncertainty in the transition state geometry in aqueous solution. The calculated fractionation factors are compared with the fractionation factors of HPO_4^{2-} and OH^- in Table 1. The reason for this comparison is that, for HPO_4^{2-} and OH^-, the experimental fractionation factors are available. Consequently, we can use our ab initio calculations for TSa and TSb to determine the relative fractionation factor of the phosphorane−Cutrpy transition state and HPO_4^{2-}. Such a relative comparison eliminates systematic errors caused by the limits of the computational protocol (this includes,

(73) Sawata, S.; Komiyama, M.; Taira, K. *J. Am. Chem. Soc.* **1995**, *117*, 2357−2358.
(74) Kresge, A. J.; More O'Ferrall, R. A.; Powell, M. F. In *Isotopes in Organic Chemistry*; Buncel, E., Lee, C. C., Ed.; Elsevier Science Publishers: New York, 1987; Vol. 7, p 256.
(75) Quinn, D. M.; Sutton, L. D. *Enzyme Mechanisms from Isotope Effects*; CRC Press: Ann Arbor, 1991.
(76) Florián, J.; Warshel, A. *J. Phys. Chem. B* **1998**, *102*, 719−734.
(77) Florián, J.; Åqvist, J.; Warshel, A. *J. Am. Chem. Soc.* **1998**, *120*, 11524−11525.

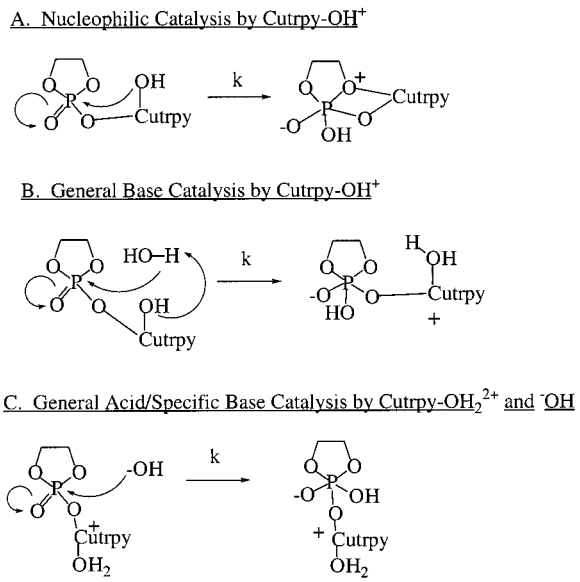

Figure 8. Proposed mechanistic steps for the Cutrpy-catalyzed hydrolysis of cAMP along with predicted solvent isotope effects (see also eqs 4−6). (A) Nucleophilic catalysis by Cutrpy-OH^+. (B) General base catalysis by Cutrpy-OH^+. (C) General acid/specific base catalysis by Cutrpy-OH_2^{2+} and OH^-. Note that chelation of the phosphorane by Cutrpy species is not indicated, but is an additional likely means of stabilizing the rate-determining transition state.

for example, the incomplete basis set) and the approximate nature of our model system. In this way we estimate the fractionation factor of phosphorane−Cutrpy transition state as $\Phi_{P-OL} = 0.82 \pm 0.10$. This value is somewhat smaller than the fractionation factor of HPO_4^{2-} because the OH group is bound less strongly in the phosphorane transition state than in HPO_4^{2-}, which results in the shift of its fractionation factor toward its value in OH^-.

Calculation of Isotope Effects. Figure 8 and eqs 5−7 illustrate our predictions, based on fractionation factors, of solvent isotope effects for mechanisms in which Cutrpy-OH^+ acts as a nucleophile (Figure 8A, eq 5), a base (Figure 8B, eq 6), or by general acid/specific base catalysis (Figure 8C, eq 7).

If a nucleophilic mechanism operates (Figure 8A), we predict a solvent isotope effect near unity (eq 5).

$$\frac{k_{H_2O}}{k_{D_2O}} = \frac{\Phi_{Cu-OL}}{\Phi_{P-OL}} = \frac{0.8 \pm 0.1}{0.82 \pm 0.1} = 1.0 \pm 0.2 \qquad (5)$$

This prediction correlates well with the measured isotope effect.

Alternatively, for a general base mechanism (Figure 8B), the solvent isotope effect involves contributions from two exchangeable protons (eq 6).

$$\frac{k_{H_2O}}{k_{D_2O}} = k_{primary} \times k_{secondary} = (4.5 \pm 2.5)\left(\frac{\Phi_{L_2O}}{\Phi_{P-OL}}\right) = 6 \pm 4 \qquad (6)$$

Here, the primary isotope effect is associated with the proton being transferred to the general base. Although there is a large uncertainty in the position of this proton in the TS, it is clear that $k_{primary} \gg 1$ for any mechanism involving proton in flight. Since the secondary isotope effect is near unity, a large positive solvent isotope effect is predicted for the general base mechanism of Figure 8B. Consequently, our measured isotope effect of 1.0 ± 0.1 certainly rules out general base catalysis by Cutrpy-OH^+.

Finally, using eq 7, we predict that general acid/specific base catalysis (Figure 8C) results in a solvent isotope effect of 0.50.

$$\frac{k_{H_2O}}{k_{D_2O}} = \frac{\Phi_{OH^-}}{\Phi_{P-OL}} = \frac{0.41}{0.82 \pm 0.1} = 0.5 \pm 0.1 \qquad (7)$$

This value would be slightly decreased if the rate-limiting step combines protonation of the leaving group by Cutrpy-OH_2^{2+} and decomposition of the phosphorane (this possibility is not explicitly indicated in Figure 8, but this process and chelation of the phorphorane by Cu are both possible). Because the measured isotope effect of 1.0 ± 0.1 is significantly larger than the isotope effect predicted using eq 7, we can rule out the general acid/specific base mechanism of Figure 8C. Another approach to rule out this mechanism was used by Kuusela and in their studies on the hydrolysis of 2′,3′-cUMP by metals.[78] Their reasoning is summarized as follows: the relative efficiencies of different metal ions in promoting the hydrolysis differ more than would be expected based on the metal-substrate binding constants. For example, Cu^{2+} and Pb^{2+} complexes of dihydrogen phosphate ion are only 1 order of magnitude more stable than the corresponding Mg^{2+} complex, but they promote the hydrolysis 10^3 times faster. In addition, the hydrolysis rate increased with increasing pH up to the pH = pK_a for the various metal aquo complexes. In fact, a linear free energy relationship was observed between the measured rate constant for the hydrolysis and the pK_a for the metal-aquo species. Thus, while substrate binding is important for hydrolysis, the acidity of the metal-bound water is the dominant property in a metal's ability to promote the reaction in these cases.

Mechanism of Hydrolysis of cAMP by Cutrpy. A comprehensive analysis of our own experiments and the relevant literature allows us to rule out mechanisms B and C with confidence and choose mechanism A (Figure 8), which corresponds to nucleophilic catalysis by Cutrpy-OH^+. In fact, nucleophilic attack by a bound copper hydroxide on an activated phosphate ester has been recently demonstrated by Burstyn and co-workers, using ^{18}O and ^{15}N isotope effects in addition to solvent isotope effects.[34] The ligand on copper in this case was 1,4,7-triazacyclononane, which generates a complex similar to Cutrpy. The measured solvent isotope effect was 1.14, which is in good agreement with our method of prediction, assuming that Cu^{II}(1,4,7-triazacyclononane) and Cutrpy have similar pK_a properties. Additionally, a similar hydrolysis involving attack by cobalt-bound hydroxide on a coordinated activated phosphate was reported by Sargeson,[79] and the measured solvent deuterium isotope effect was 1.2.

As depicted in Figure 8, we propose that the cAMP substrate is activated toward nucleophilic attack by association of the cyclic phosphate with Cutrpy. This is consistent with the observation that metals are much more efficient at promoting the hydrolysis than are organic buffers of similar pK_a. We conclude that our measured solvent isotope effect rules out a general base mechanism by Cutrpy-OH^+. The data are most consistent with a mechanism in which Cutrpy-OH^+ behaves as a nucleophile.

It is important to note that protonation of the 2′- or 3′-oxygen leaving group is required at the pH values for which we investigated cAMP hydrolysis. This regenerates metal hydroxide and completes the catalytic cycle. In fact, a proton transfer from

(78) Kuusela, S.; Lönnberg, H. *J. Phys. Org. Chem.* **1992**, *5*, 803−811.
(79) Jones, D. R.; Lindoy, L. F.; Sargeson, A. M. *J. Am. Chem. Soc.* **1983**, *105*, 7327−7336.

Cutrpy-OH_2^{2+} is required for a complete catalytic cycle. We propose that Cutrpy-OH_2^{2+} can act as a Brønsted acid and protonate the leaving group. A coordinated water molecule that substitutes for the departing Cu-OH nucleophile may serve this purpose. Alternatively, the metal center may assist the leaving oxygen, and facilitate proton transfer via solvent water molecules.

Conclusions

We previously showed that Cutrpy transesterifies RNA and generates 2′,3′-cyclic phosphates.[22,43,47,48,51−54,78] Here, we demonstrated that the metal complex Cu(II)terpyridine catalyzes the hydrolysis of adenosine 2′,3′-cyclic monophosphate. The proposed mechanism involves prior association of the phosphate and the metal (most likely simple metal−phosphate coordination), and nucleophilic catalysis by Cutrpy-OH^+. Brønsted acid catalysis by metal-bound waters has rarely been proposed as a possible reaction mechanism,[27,80] but we suggest that Cutrpy-OH_2^{2+} is an effective Brønsted acid in this system which undergoes proton transfer to regenerate the catalyst, Cutrpy-OH^+. This nucleophilic attack by a metal-bound hydroxide mechanism bears similarity to the attack by Mg alkoxide recently reported for a hammerhead ribozyme.[73] We recommend against the use of NaCl as an ionic strength buffer for reactions of Cu(II) complexes and related metal complexes with RNA.

Acknowledgment. L.A.J. was a Dean's Fellow for 1994-95. This work was supported in part by NSF Grants CHE-9318581 and CHE-9802660 to J.K.B. and NSF Grant MCB-9808638 to A.W. Acknowledgment is made to the donors of the Petroleum Research Fund, administered by the American Chemical Society, for partial support of this research in the J.K.B. group. We thank Professor Wesley Harris for helpful discussions on speciation behavior and the SPE program.

IC990228R

(80) Suh, J. *Acc. Chem. Res.* **1992**, *25*, 273−279.
(81) Florián, J.; Warshel, A. *J. Phys. Chem. B* **1997**, *101*, 5583−5595.
(82) Florián, J.; Warshel, A. *ChemSol*, Version 1.0; University of Southern California: Los Angeles, 1997.